doi:10.1016/j.jmb.2004.09.053 J. Mol. Biol. (2004) 344, 481–493

JMB

Available online at www.sciencedirect.com

SCIENCE DIRECT®

ELSEVIER

Molecular Control of a Bimodal Distribution of Quinone-Analogue Inhibitor Binding Sites in the Cytochrome b_6f Complex

Jiusheng Yan* and William A. Cramer*

Department of Biological Sciences, Lilly Hall of Life Sciences, Purdue University 915 W. State Street, West Lafayette, IN 47907-2054 USA

**Corresponding authors*

The 3.0–3.1 Å X-ray structures of the cytochrome b_6f complex from *Mastigocladus laminosus* and *Chlamydomonas reinhardtii* obtained in the presence of the p-side quinone-analogue inhibitor tridecyl-stigmatellin (TDS) are very similar. A difference occurs in the p-side binding position of TDS. In *C. reinhardtii*, TDS binds in the ring-in mode, as previously found for stigmatellin in X-ray structures of the cytochrome bc_1 complex. In this mode, the H-bonding chromone ring moiety of the TDS bound in the Q_p niche is proximal to the ISP [2Fe–2S] cluster, and its 13 carbon tail extends through a portal to the large inter-monomer quinone-exchange cavity. However, in *M. laminosus*, TDS binds in an oppositely oriented ring-out mode, with the tail inserted toward the Q_p niche through the portal and the ring caught in the quinone-exchange cavity that is 20 Å away from the [2Fe–2S] cluster. Site-directed mutagenesis of residues that might determine TDS binding was performed with the related transformable cyanobacterium *Synechococcus* sp. PCC 7002. The following changes in the sensitivity of electron transport activity to TDS and stigmatellin were observed: (a) little effect of mutation L193A in cytochrome b_6, which is proximal to the chromone of the ring-out TDS; (b) almost complete loss of sensitivity by mutation L111A in the ISP cluster binding region, which is close to the chromone of the ring-in TDS; (c) a ten and 60-fold increase associated with the mutation L81F in subunit IV. It was inferred that only the ring-in binding mode, in which the ring interacts with residues near the ISP, is inhibitory, and that residue 81 of subunit IV, which resides at the immediate entrance to the Q_p niche, controls the relative binding affinity of inhibitor at the two different binding sites.

Keywords: quinone exchange cavity; Rieske iron–sulfur protein; *Synechococcus* sp. PCC 7002; stigmatellin; transporter

Introduction

The structures of respiratory and photosynthetic cytochrome *bc* complexes provide unique information on the pathway and mechanism of transfer of the hydrophobic substrate, lipophilic quinone, between the bulk lipid phase and the reaction sites in the membrane protein complex. The structures of the dimeric b_6f complex from the thermophilic cyanobacterium, *Mastigocladus laminosus*,[1] and the green alga, *Chlamydomonas reinhardtii*,[2] in the presence of the p-side quinone analogue inhibitor tridecyl-stigmatellin (TDS), have been resolved by X-ray crystallography to 3 Å and 3.1 Å (Protein Data Bank ID, 1VF5 and 1Q90, respectively) (Figure 1(A)). Several features of these structures have been reviewed recently.[3–5] This integral membrane protein complex in oxygenic photosynthetic membranes mediates electron transfer from photosystem II to photosystem I. It oxidizes a lipophilic molecule, plastoquinol

Abbreviations used: TDS, tridecyl-stigmatellin; I_{50}, concentration of inhibitor that reduces activity to 50%; ISP, iron–sulfur protein; n- and p-, electrochemically negative and positive sides of the membrane with reference of the proton gradient; PQ, plastoquinone; Q_p, p-side quinone binding site; WT^S, *Synehcococcus* strain with a wild-type b_6f complex that is resistant to spectinomycin; WT^{HSK}, strain with a His-tagged cytochrome *f* that is resistant to spectinomycin and kanamycin.

E-mail addresses of the corresponding authors: yanjiush@bilbo.bio.purdue.edu; wac@bilbo.bio.purdue.edu

0022-2836/$ - see front matter

(chemical structure shown in Figure 1(B)), and reduces a soluble copper or heme protein, plastocyanin or cytochrome c_6, by a "Q-cycle" mechanism that establishes an electrochemical proton gradient across the membrane.[6–14] The b_6f complex is analogous to the cytochrome bc_1 complex of mitochondria and purple photosynthetic bacteria, as both function as an "electron transporter and proton pump" and both contain a cytochrome b/b_6 with two *b*-type hemes, a Rieske iron–sulfur protein (ISP) with one [2Fe–2S] cluster, and a cytochrome c_1/f containing a *c*-type heme.[4,15,16]

The b_6f complex is composed of eight subunits with 13 trans-membrane helices, two large extramembrane soluble domains, and seven natural prosthetic groups in each monomer (Figure 1(A)). The structures of cytochrome b_6 and subunit IV are very similar to the N and C-terminal halves of the cytochrome *b* subunit in the bc_1 complex, as predicted from homology of sequence and hydropathy plots.[17] Cytochrome *f* and the ISP, each of which has a large extramembrane soluble domain and single transmembrane helix, are similar in the location of the transmembrane helical domain to their analogue subunit in the bc_1 complex. However, the position of the heme of cytochrome *f* is shifted by ~16 Å relative to that of cytochrome c_1.[18–22] In addition, three prosthetic groups, chlorophyll *a*, β-carotene, a newly discovered covalently bound heme, and the peripheral four small hydrophobic subunits (PetG, PetL, PetM and PetN) are absent in the bc_1 complex.

The structures of the b_6f complex from *M. laminosus* and *C. reinhardtii* are remarkably similar,[1,2] although there were approximately one billion years between the appearance of these organisms on the Earth.[23] Despite the discrepancy in the assignment of the identities of three small subunits, their 3D structures are essentially identical in all of the subunits, cytochrome *f*, cytochrome b_6, subunit IV, the four small subunits, and the ISP transmembrane domain (Figure 1(A)), with a root mean square deviation (RMSD) of 1.27 Å for C^{α} atoms of most (94%) residues in these components. However, a major difference occurs in the p-side binding position of the inhibitor, TDS (Figure 1). In *C. reinhardtii*, TDS binds in a ring-in mode, as previously found for stigmatellin (chemical structure shown in Figure 1(B)) in the structures of the respiratory cytochrome bc_1 complex.[19,21,22] In this mode, the ring moiety of the TDS is bound proximal to the ISP [2Fe–2S] cluster in a Q_p niche, allowing formation of an H-bond between ISP-His126 (one of two His ligands of the [2Fe–2S] cluster) and the O4 of the TDS chromone ring, while the 13 carbon tail of the TDS extends through the portal from the Q_p niche to the inter-monomer quinone exchange cavity which exchanges quinone with the membrane bulk lipid phase (Figures 1(A), 2A, and 3). In *M. laminosus*, however, TDS binds in a novel ring-out mode, with its tail inserted in the opposite direction into the portal and the chromone ring bound at the roof of the quinone exchange cavity that is 20 Å from the His-ligand of the [2Fe–2S] cluster (Figures 1(A), 2B, and 3). This unusual orientation of TDS could be peculiar to the particular crystallization regime. Alternatively, it could reflect a different binding configuration of this inhibitor in the cyanobacterial cytochrome b_6f complex and, thereby, either a different mode of inhibition or an intermediate bound-state of the translocated quinone.

Using the transformable cyanobacterium *Synechococcus* sp. PCC 7002 as a model, the role of key residues that might determine the binding of TDS was investigated by site-directed mutagenesis. The consequences for inhibitor sensitivity were assayed through their effects on the reduction kinetics of cytochrome f/c_6 in intact cells. The results implied that: (i) inhibition by TDS results primarily from the ring-in binding mode; (ii) the identity of subunit IV residue 81 is critical for the relative binding affinity of TDS at the ring-in and ring-out binding sites; (iii) the ring-out configuration is inferred to be an intermediate in transfer of quinone between the large quinone exchange cavity and Q_p niche.

Results

Comparison of the TDS binding pockets in the *C. reinhardtii* and *M. laminosus* b_6f complexes

The binding of TDS in the ring-out mode found in *M. laminosus* appears to have little influence on the ISP domain movement or the overall structure of the Q_p site because no significant difference was observed in the structure of the 3.0 Å TDS-b_6f complex relative to the 3.4 Å structure of the native complex.[1] However, compared to the *M. laminosus* structure, the Q_p-niche of the TDS-b_6f complex of *C. reinhardtii* was enlarged by ~2 Å to accommodate the TDS ring, and its [2Fe–2S] cluster binding region was inserted 4 Å deeper into the membrane phase to allow the formation of an H-bond between ISP-His155 (one of the two His ligands of the [2Fe–2S] cluster) and O4 of the TDS chromone ring (Figures 2A and B, and 3). Such a structure change is likely a consequence of the TDS binding in the ring-in mode, as a similar enlargement of the Q_p-niche was also observed in the bc_1 complex upon stigmatellin binding.[19,21,22]

The chlorophyll phytol chain also extends into the Q_p portal with different orientations in the two structures. In the TDS-b_6f complex of *M. laminosus*, the phytol chain is in a bent-down conformation in which the chain is bent away from the TDS and packed around the F helix of subunit IV (Figures 1(A), 2B, and 3). However, in the TDS-bound *C. reinhardtii* structure, the phytol chain has an altered bent-up conformation in which the chain is rotated by ~180° relative to the bent-down conformation and is aligned parallel (within 4–5 Å) to the tail of the ring-in TDS conformation (Figures 1(A), 2A, and 3). In the

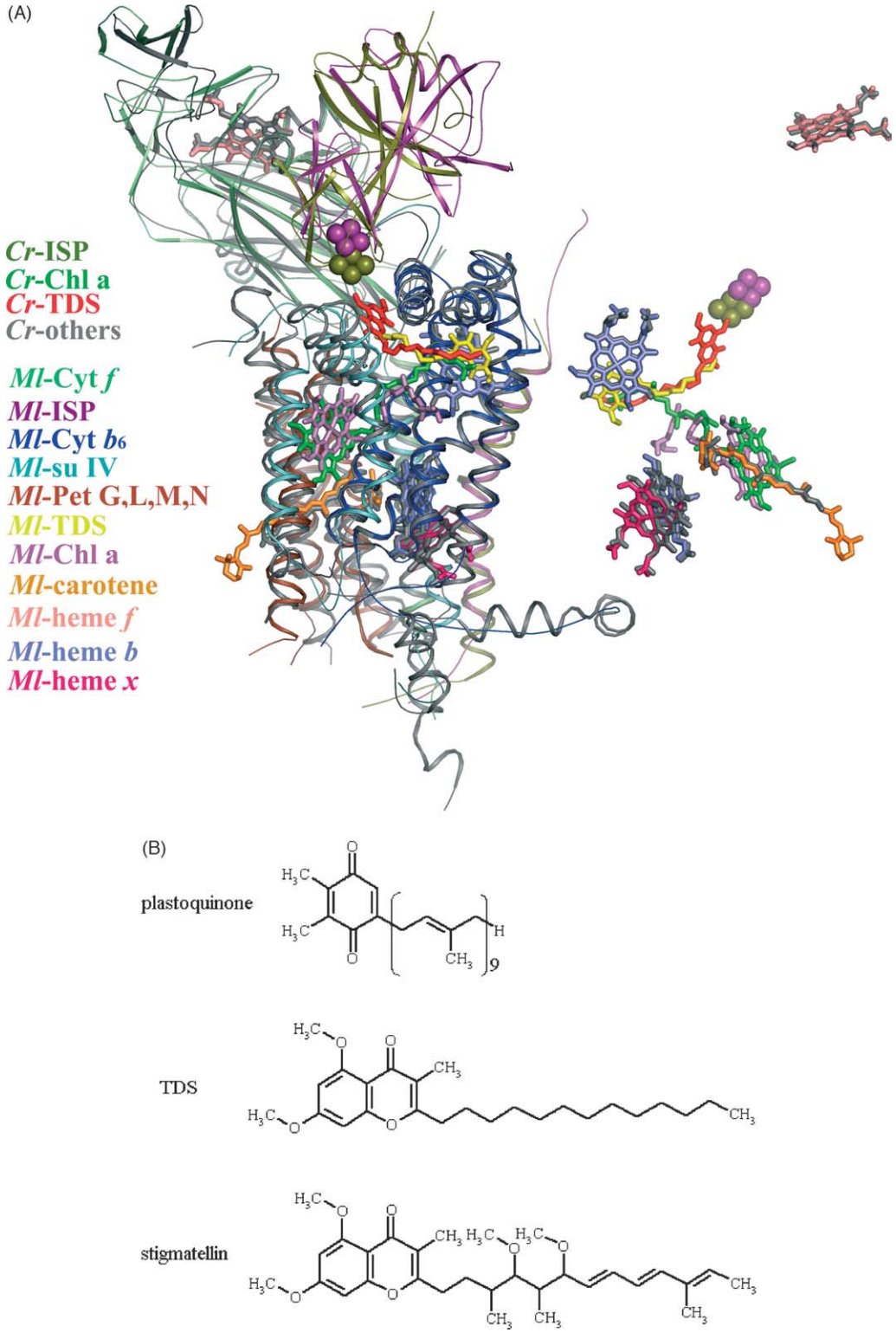

Figure 1. (A) Structure comparison of the TDS-bound b_6f complexes from *M. laminosus* and *C. reinhardtii*. The two structures were superimposed with the "iterative magic fit" tool of program Swiss-PDBViewer. All components are shown in one monomer and only the TDS and prosthetic groups in the other monomer. The *C. reinhardtii* complex is shown in grey with the exceptions that the ISP is in olive, TDS in red and chlorophyll *a* in green. The color code for *M. laminosus* complex is: lime, cytochrome *f*; purple, ISP; blue, cytochrome b_6; cyan, subunit IV; brown, small subunits; yellow, TDS; slate, *b*-hemes; hot-pink, heme *x*; salmon, *f*-heme; orange, β-carotene; violet, chlorophyll. The [2Fe–2S] clusters of the ISP are shown as spheres. All structural Figures were drawn with program PyMol (http://pymol.sourceforge.net). (B) Chemical structures of plastoquinone, TDS, and stigmatellin.

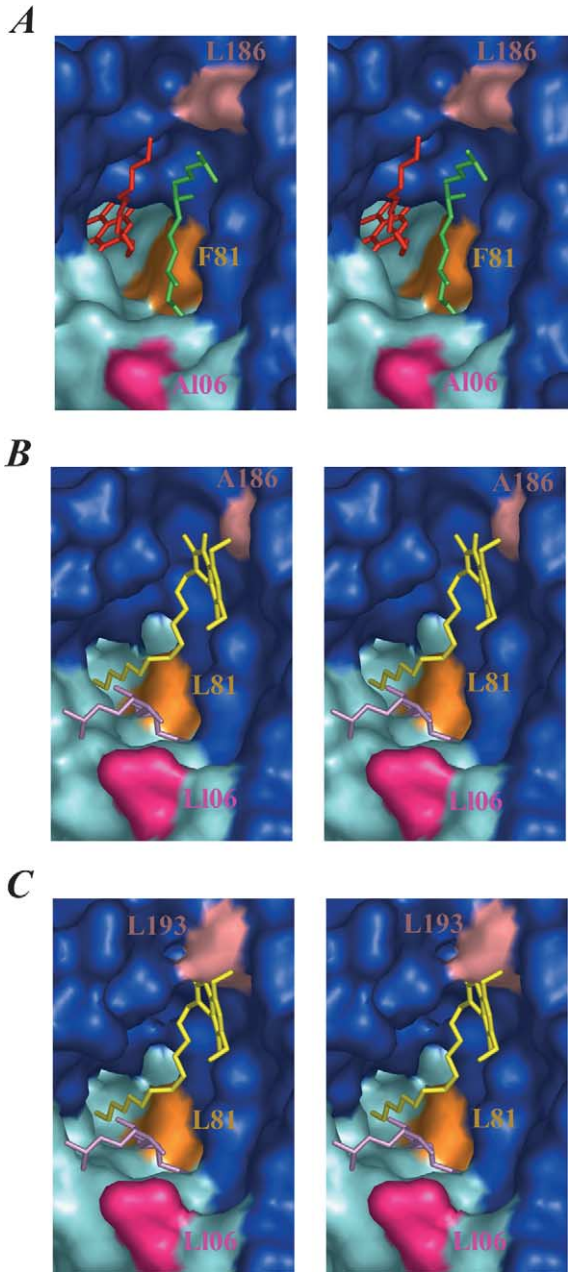

Figure 2. Surface view (stereo pairs) of the TDS and chlorophyll phytol chain binding pockets from the quinone exchange cavity. A, The ring-in-TDS and bent-up-phytol chain binding pocket in *C. reinhardtii*; B, the ring-out-TDS and bent-down-phytol chain binding pocket in the *M. laminosus*; and C, the modeled structure of the ring-out-TDS and bent-down-phytol chain binding pocket in the *Synechococcus* sp. PCC 7002 based on the *M. laminosus* structure. Color code: blue surface, cytochrome b_6; cyan surface, subunit IV; red sticks, ring-in-TDS; yellow sticks, ring-out-TDS; green sticks, bent-up phytol chain; violet sticks, bent-down-phytol chain; salmon surface, residue 186 (193 for *Synehcococcus* sp. PCC 7002) of cytochrome b_6; orange surface, residue 81 of subunit IV; hot-pink surface, residue 106 of subunit IV.

superimposed structure (Figure 3), this bent-up conformation of the phytol chain occupies part of the space that is occupied by the *M. laminosus* ring-out TDS ring and the first six carbon atoms of the tail, suggesting a possible steric role of the phytol chain in the control of the TDS binding in the two different modes.

The molecular basis for the difference in TDS binding can be sought in the amino acid residue differences between *M. laminosus* and *C. reinhardtii* structures that define the TDS and the phytol chain binding pockets. The 39 amino acid residues that reside within 5 Å of the TDS and the chlorophyll phytol chain in the 3.0–3.1 Å structures from *M. laminosus* and *C. reinhardtii* are summarized (Table 1(A) and (B)). The homologous sequences from a higher plant (spinach) and other cyanobacteria, particularly *Synechococcus* sp. 7002, which was used for mutagenesis analysis in this study, are also shown. Among these residues, only four are different in amino acid sequence between *M. laminosus* and *C. reinhardtii* (Table 1(A) and (B)). (i) Residue 81 of subunit IV, which is located at the start of the p-side small *ef*-helix, is conserved as a Leu in cyanobacteria, but is replaced by a Phe in green algae and higher plants. The residues at this position are at the immediate entrance to the Q_p-niche, and are close to both the TDS (3–5 Å to the start of the ring-in-TDS tail or the end of the ring-out-TDS tail) and the chlorophyll phytol chain (3–4 Å to the start of both bent-up and bent-down chlorophyll phytol chains) (Figures 2A and B, and 3). (ii) Residue 186 of the D-helix in cytochrome b_6 is an Ala, which is 3 Å from the ring-out-TDS ring in *M. laminosus*, and is substituted by a Leu in *C. reinhardtii* (Table 1; Figures 2A and B, and 3). This Leu or Ala is also 4–5 Å from the end of the bent-up chlorophyll phytol chain. (iii) Residue 106 of the F-helix of subunit IV is a Leu in *M. laminosus* and an Ala in *C. reinhardtii*. The Leu is close (4 Å) to the end of chlorophyll phytol chain in *M. laminosus* and might have a role in stabilization of the phytol chain in the bent-down conformation through van der Waals interactions (Figures 2B and 3). (iv) A difference also occurs at position 183 of cytochrome b_6, which is Tyr in *M. laminosus* but Phe in *C. reinhardtii*. While the three differences (i, ii, and iii) may have a steric effect on the relative propensity for a ring-in or ring-out orientation of TDS through the portal, or for a bent-down or bent-up conformation of chlorophyll phytol chain, the effect of the difference (iv) at residue 183 of cytochrome b_6 appears to be negligible because the hydroxyl group of the Tyr does not make hydrogen bond to TDS (Figure 3).

TDS binding in *Synechococcus* sp. PCC 7002: only the ring-in mode is inhibitory for the b_6f complex

To study the inhibitory role and the molecular basis for the control of the two different TDS binding modes, site-directed mutagenesis of

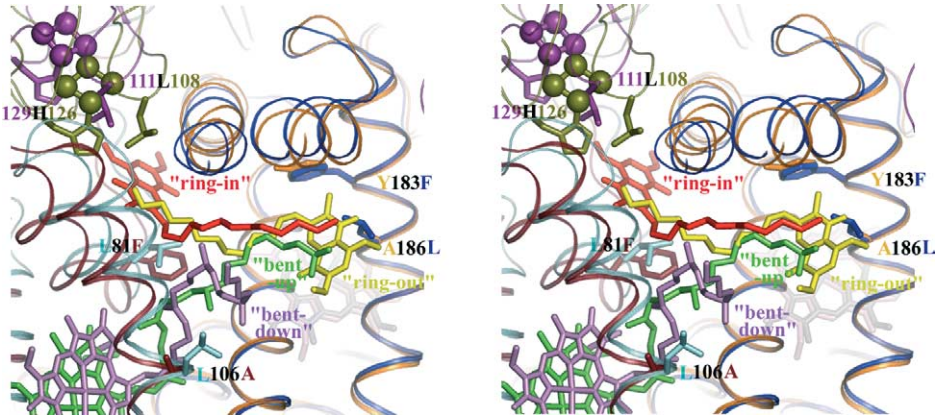

Figure 3. Structural comparison of the TDS binding pockets in the *M. laminosus* (*Ml*) and *C. reinhardtii* (*Cr*) b_6f complexes. The two structures were superimposed as in Figure 1(A). The color code is: yellow, *Ml*-ring-out TDS; red, *Cr*-ring-in TDS; violet, *Ml*-chlorophyll; green, *Cr*-chlorophyll; orange, *Ml*-cytochrome b_6; blue, *Cr*-cytochrome b_6; cyan, *Ml*-subunit IV; ruby, *Cr*-subunit IV; purple, *Ml*-ISP; olive, *Cr*-ISP; pink, *Ml*-heme b_p; grey, *Cr*-heme b_p. Residues discussed in this study are shown in sticks. To be consistent with the residue ID numbers in *M. laminosus* structure (PDB:1VF5), the residue ID numbers for the *Cr*-ISP are renumbered to exclude the N-terminal 29 residue signal peptide which is counted in *C. reinhardtii* structure coordinate file (PDB:1Q90).

residues that may affect the TDS binding was performed with the transformable cyanobacterium *Synechococcus* sp. PCC 7002. The b_6f complex in this organism has a higher degree of homology to *M. laminosus* complex (identity = 73.6% for the four large subunits), than to *C. reinhardtii* complex (identity = 66.1%). Furthermore, as in *M. laminosus*, *Synechococcus* sp. PCC 7002 also has a Leu at both positions 81 and 106 of subunit IV. Therefore, it is assumed that as in *M. laminosus*, TDS also preferably binds in a ring-out mode and the chlorophyll phytol chain adopts a bent-down conformation in the *Synechococcus* b_6f complex (Figure 2C). Flash kinetic experiments to measure the rate of cytochrome *f* reduction with *M. laminosus* cells *in vivo* indicated that the electron transfer activity of the b_6f complex in this organism can also be inhibited by TDS as in *Synechococcus* (data not shown); however, an accurate titration of the inhibitor sensitivity in *M. laminosus* could not be obtained because of a high content of phycobiliproteins that create spectral interference.

It is noted that *Synechococcus* is different from all the other organisms listed in Table 1 at four positions: G132-T133 of cytochrome b_6 and Q101-G102 of subunit IV. However, residues at these

Table 1. Amino acid sequence alignment of the residues within 5 Å of (A) ring-out-TDS and bent-down-chlorophyll phytol chain in *M. laminosus*, and (B) ring-out-TDS and bent-up-chlorophyll phytol chain in *C. reinhardtii*

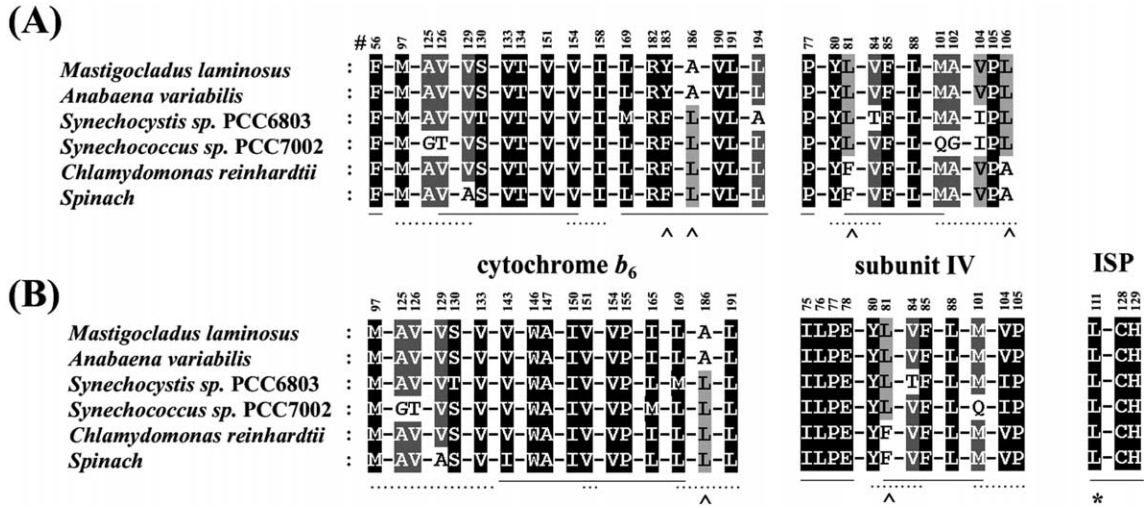

Residue identification numbers are valid for most sequences except that *Synechocystis* sp. PCC6803 and *Synechococcus* sp. PCC7002 have seven more residues at their N terminus of cytochrome b_6, and *C. reinhardtii* and spinach, respectively, have three and one less residues at their N terminus of the ISP. —, Residues that are close to TDS. …, Residues that are close to phytol chain. ^, Residues that are different between *M. laminosus* and *C. reihardtii*. *, Residues that were also of interest in this study.

positions are believed to be unimportant in the control of TDS binding modes because *C. reinhardtii* and *M. laminosus* have identical residues at these four positions: A125-V126 of cytochrome b_6 and M101-A102 of subunit IV. The only important sequence difference between the *M. laminosus* and *Synechococcus* that could affect the TDS and phytol chain binding pockets, is at residue 186 of cytochrome b_6 which is an Ala in *M. laminosus*, but a Leu in *Synechococcus* sp. PCC 7002 (residue 193) and *C. reinhardtii* (Table 1, Figure 2). As seen in the superimposed structures of *M. laminosus* and *C. reinhardtii* (Figure 3) and the modeled structure of the TDS binding pocket in *Synehcococcus* sp. PCC 7002 (Figure 2C), this Leu residue is 7 Å or 14 Å away from the ring-in TDS tail or chromone ring, but it partly overlaps with the ring-out-TDS ring. Thus, it is anticipated that the presence of a bulky Leu residue at this position in *Synechococcus* and *C. reinhardtii* would have no influence on the binding of TDS in the ring-in mode, but might decrease the binding affinity of TDS in the ring-out mode. However, mutation of this Leu to Ala (mutant b_6-L193A) in *Synechococcus* sp. PCC 7002 had no significant effect on the sensitivity of the b_6f complex to either TDS or stigmatellin (Table 2, Figure 4). This implies that either (i) this mutation had no influence on the TDS binding in the ring-out mode, or (ii) this mutation increased the TDS binding affinity in the ring-out mode, but this binding mode is undetectable in the activity assay, i.e. not effective for inhibition of electron transfer activity. If possibility (i) applies, there should be no significant difference in the TDS binding mode in *M. laminosus* and *Synechococcus*, and thus a ring-out binding mode of TDS must also exist in *Synechococcus*. However, as discussed below, this also leads to the conclusion that the ring-out binding mode is not inhibitory.

In order to define the inhibition efficiency of the two TDS binding modes, two mutants of residue Leu111 of the ISP were constructed. This residue is located in the [2Fe–2S] cluster binding motif (Figure 3), and fully conserved in both b_6f (Table 1(B)) and bc_1 complexes. It is close (within 3–5 Å) to the TDS ring in the ring-in mode in both the bc_1[19,22] and *C. reinhardtii* b_6f complex,[2] but far (17 Å) away from the TDS ring in the ring-out mode in the *M. laminosus* complex[1] (Figure 3). It was shown in the *Rb. capsulatus* bc_1 complex that mutation of the equivalent Leu (residue 136 of cytochrome *b*) to Ala or Tyr led to a high stigmatellin resistance.[24] It is therefore expected that mutation of this residue should also have a significant effect on TDS binding in the *C. reinhardtii* ring-in mode, but would exert little change in TDS binding affinity in the *M. laminosus* ring-out mode. It was observed in *Synechococcus* sp. PCC 7002 that mutation of this residue to Ala (mutant ISP-L111A) led to an almost complete loss of sensitivity to TDS (Table 2, Figures 5A and 6A) and stigmatellin (Table 2, Figure 6B), and to Tyr (mutant ISP-L111Y) resulted in a more than tenfold decrease in sensitivity to both inhibitors (Table 2, Figure 6A and B). This indicates a critical role of residue ISP-Leu111 in the binding of TDS or stigmatellin in the ring-in mode, which requires interaction of the inhibitor with the ISP [2Fe–2S] cluster binding domain. Therefore, it is inferred that only the ring-in binding mode is responsible for the inhibition by TDS and stigmatellin, and the ring-out binding mode, if it exists as inferred from the possibility (i) above, is not inhibitory in *Synechococcus* sp. PCC 7002.

The mutation ISP-L111A/Y also resulted in a 42($\pm$6)% or 32($\pm$6)% decrease in electron transfer activity, relative to the spectinomycin-resistant wild-type (WT^S, $k_{ET}=191(\pm23)\ s^{-1}$) (Table 2), which might be due to a decrease in the redox potential of the [2Fe–2S] cluster as in the *Rb. capsulatus* bc_1 complex,[24] and/or an alteration in the Q_p site. It was shown in the *Rb. capsulatus* bc_1 complex that all four other mutations (R, H, D, and G) of the equivalent Leu (residue 136) resulted in an almost complete (95%) loss of the enzyme activity and impaired interactions with both UQ/UQH2 and stigmatellin.[25] These results indicate that a Leu residue at this position is specifically required for

Table 2. Properties of *Synechococcus* sp. PCC 7002 wild-type and mutant strains

Strains	k_{ET} (s^{-1}) (no inihibitor)	I_{50} (nM) TDS	I_{50} (nM) Stg	Notes
WT^{HSK}	92$\pm$5	150	500	Wild-type of b_6f complex; His-tagged at C terminus of cytochrome *f*; resistant to spectinomycin and kanamycin
IV-L81F	123$\pm$10	15	8	His-tagged at C terminus of cytochrome *f*; resistant to spectinomycin and kanamycin
IV-L81A	79$\pm$5	200	70	His-tagged at C terminus of cytochrome *f*; resistant to spectinomycin and kanamycin
b_6-L193A	120$\pm$18	200	350	His-tagged at C terminus of cytochrome *f*; resistant to spectinomycin and kanamycin
WT^S	191$\pm$23	50	150	Wild-type of b_6f complex; resistant to spectinomycin
ISP-L111A	111$\pm$11	INS	INS	Resistant to spectinomycin
ISP-L111Y	129$\pm$8	3000	3000	Resistant to spectinomycin

k_{ET}, electron transfer rate from plastoquinol to cytochrome f/c_6, measured by the rate of flashed-induced reduction of cytochrome f/c_6 in intact cells. Stg, stigmatellin; I_{50}, concentration of the inhibitor that reduces enzyme activity to 50%; INS, insensitive.

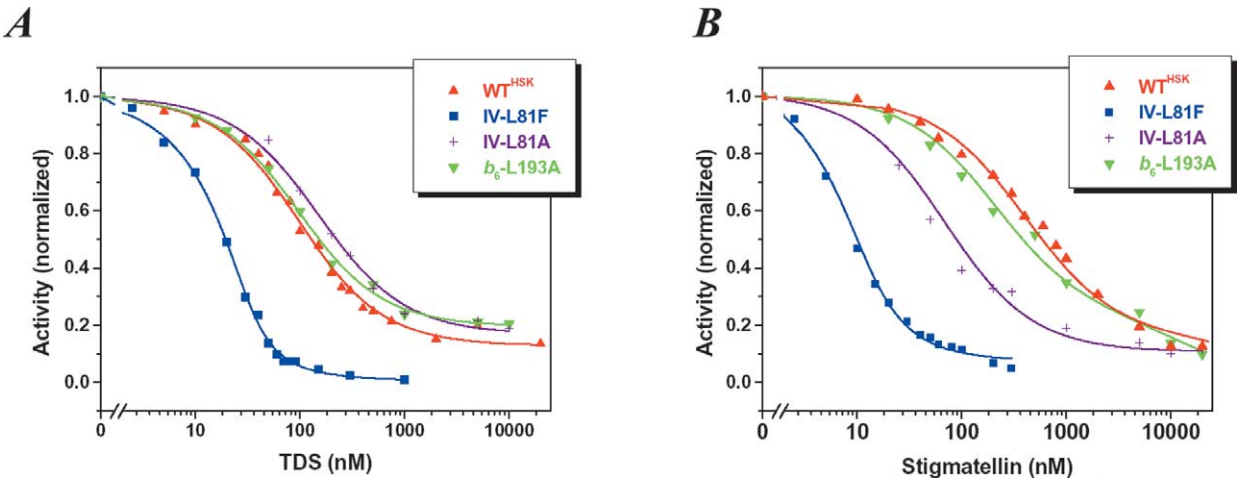

Figure 4. Inhibitory effects of (A) TDS and (B) stigmatellin on the electron transfer activity of the b_6f complex as measured by the flash-induced re-reduction rate of cytochrome f/c_6 in intact cells of WT^{HSK}, b_6-L193A, and IV-L81F. Activity is normalized to the rate in the absence of inhibitor (see Table 2).

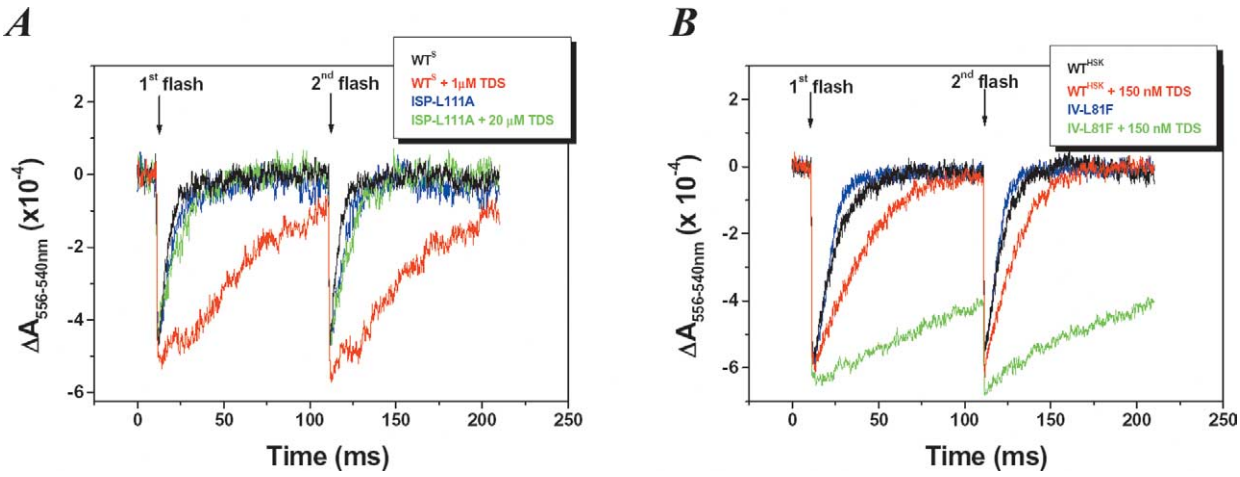

Figure 5. Flash-induced oxidation–reduction of cytochrome f/c_6 in intact cells of (A) WT^S and ISP-L111A and of (B) WT^{HSK} and IV-L81F, in the absence/presence of TDS. Two cycles of oxidation–reduction are shown.

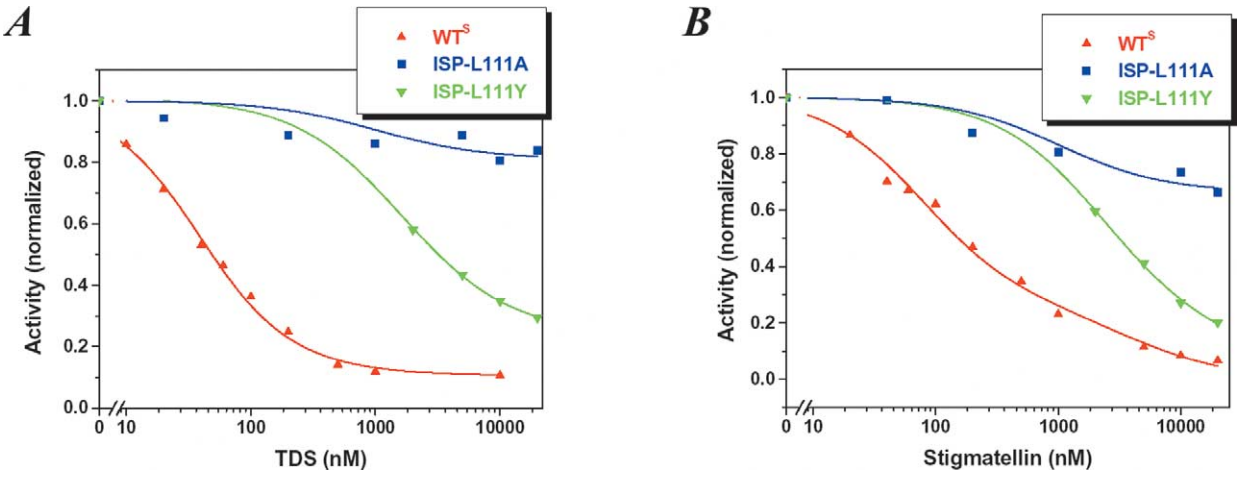

Figure 6. Inhibitory effects of (A) TDS and (B) stigmatellin on the electron transfer activity of the b_6f complex measured by the rate of flash-induced re-reduction of cytochrome f/c_6 in intact cells of WT^S, ISP-L111A, and ISP-L111Y. Activity is normalized as in Figure 4.

efficient binding of quinol substrate or stigmatellin at the Q_p site. This Leu residue may affect substrate or inhibitor binding at the Q_p niche through direct van der Waals interactions because of its proximity (3–5 Å) to the chromone ring of the ring-in stigmatellin and TDS as seen in crystal structures of the bc_1 and b_6f complexes.[1,2,19,21,22] Alternatively, it may control docking of the [2Fe–2S] cluster binding region to the cytochrome b_6/subunit IV at the Q_p site. A proper docking of the [2Fe–2S] cluster binding region is required for the TDS or stigmatellin binding in the ring-in mode. This latter mechanism is consistent with our previous report[26] that changes in the length of the ISP hinge region affected the inhibitor sensitivity of the b_6f complex to stigmatellin by altering ISP docking at the Q_p site.

Residue 81 of subunit IV has a critical role in controlling the TDS binding affinity

All cyanobacteria have a Leu at position 81 of subunit IV, while it is replaced by a Phe in all green algae and higher plants (Table 1). Mutation of the IV-L81 to Phe in *Synechococcus* PCC 7002 resulted in only a small (30%) increase in the electron transfer activity of the b_6f complex (Table 2, Figure 5B), but a ~ten and ~60-fold increase, respectively, in sensitivity to TDS (Table 2; Figures 4A and 5B) and stigmatellin (Table 2; Figure 4B). In the control strain (WT^{HSK}), the I_{50} for the inhibition of the flash-induced reduction was approximately 150 nM and 500 nM, respectively, for TDS and stigmatellin. However, in the mutant IV-L81F, the I_{50} was decreased to 15 nM and 8 nM for TDS and stigmatellin, respectively. This result implies that the b_6f complex in algae and higher plants is significantly more sensitive to TDS and stigmatellin than in cyanobacteria. This is presumably a consequence of the difference in TDS binding modes observed for *M. laminosus* and *C. reinhardtii*. A Leu→Phe change at residue 81 of subunit IV increases the TDS binding affinity in the inhibitory ring-in binding mode, and may also decrease affinity for TDS binding in the non-inhibitory ring-out mode.

In the superimposed structures (Figure 3), the side-chain of subunit IV-L81 in one monomer of the *M. laminosus* structure is slightly (1–1.5 Å) closer to the bound TDS than is that of IV-F81 in *C. reinhardtii* (Figure 3). To study the possibility that a Leu residue at this position may partially occlude the Q_p niche and thus decrease binding affinity of the TDS in the ring-in mode, this residue was mutated to the small residue, Ala. Both the electron transfer rate of the b_6f complex and its sensitivity to TDS in this IV-L81A mutant were not significantly changed compared to WT^{HSK} (Table 2; Figure 4A). This suggests that it is mainly the aromaticity of the Phe at residue 81 of subunit IV, rather than the availability of space at this position, that stabilizes the binding of TDS in the ring-in mode. However, the sensitivity to stigmatellin is increased by ~sixfold (Table 2; Figure 4B) in this IV-L81A mutant, suggesting a steric effect of the IV-Leu81 residue on the stigmatellin binding. This is consistent with the fact that stigmatellin has a more bulky tail than TDS (Figure 1(B)). In the crystal structure of the yeast bc_1 complex (PDB ID, 1EZV),[22] the first side-chain (methyl group) of the stigmatellin tail is close (4 Å) to the equivalent Leu residue (Leu275 of cytochrome *b*).

Discussion

Quinone binding in the Q_p pocket: the first example of two binding modes for a quinone analogue inhibitor

In the bc_1 complex, the binding sites of Q_p site inhibitors, azoxystrobin, myxothiazol, (*E*)-β-methoxyacrylate (MOA)-stilbene, stigmatellin, 5-undecyl-6-hydroxy-4,7-dioxobenzothiazol (UHDBT), 5-*n*-heptyl-6-hydroxy-4,7-dioxobenzothiazole (HHDBT), 2-nonyl-4-hydroxyquinoline *N*-oxide (NQNO), and famoxadone, have been resolved by X-ray crystallographic analysis.[18,19,21,22,27–29] These inhibitors define a large p-side quinone-binding (Q_p) space, in which the head groups of these inhibitors reside in a Q_p pocket, and the tails (if present) extend into the Q_p-portal toward the quinone-exchange cavity. From the Q_p pocket, quinol substrate can be oxidized and deprotonated with one of its electrons transferred to ISP, the other to heme b_p and the two protons discharged into the p-side water phase. In the Q_p pocket, the MOA group of the first three inhibitors is bound at a site proximal to the heme b_p, and the reactive quinone ring of the next four inhibitors is caught at a distal site that is close to the ISP [2Fe–2S] cluster. The three aromatic rings of the famoxadone span both proximal and distal sites. The finding of a ring-out binding mode of TDS in the *M. laminosus* complex is the first observation of a bimodal binding of an inhibitor acting in the Q_p space.

The ring-in binding mode of TDS observed in *C. reinhardtii*[2] (Figures 1(A), 2A, and 3) is similar to that documented for the binding of stigmatellin to the mitochondrial cytochrome bc_1 complex,[19,21,22] where the mechanism of inhibition is attributed to displacement of the physiological ubiquinol that is H-bonded to the Rieske ISP.[30–32] However, in *M. laminosus*,[1] the H-bond reactive quinone ring of the TDS in the novel ring-out binding mode is outside the Q_p pocket and 20 Å from the reactive histidine of the ISP (Figures 1(A), 2B, and 3). It had been proposed that the TDS bound in this ring-out mode could inhibit the complex by occlusion of the portal, which would make movement of the plastoquinone through the portal a rate-limiting step.[1] However, as shown in this study, the inhibitory effect of the TDS and stigmatellin can be almost fully abolished by a mutation (ISP-L111A), which is expected to affect TDS binding in the ring-in but not ring-out binding mode. On the other hand, the mutation b_6-L193A, which is

expected to increase the binding affinity of the TDS in the ring-out mode, had no significant effect on inhibition of the complex by TDS and stigmatellin (Table 2; Figure 4). Thus, it is inferred that TDS bound in the ring-out mode is not inhibitory, and only the ring-in binding mode is inhibitory for the turnover of the b_6f complex. The observed inhibitory effect of TDS in *M. laminosus* or the *Synechococcus* b6-L193A mutant must arise from TDS bound in the ring-in binding mode. In these two cyanobacteria, the ring-in binding site must be a low affinity site compared to the non-inhibitory ring-out binding site, because only the latter mode is observed in the *M. laminosus* structure.[1]

Molecular basis for the control of TDS binding in the two different modes: possible roles of subunit IV residue 81 and the chlorophyll phytol chain

The TDS binding pocket for both the ring-in and ring-out modes is very similar in the *M. laminosus* and *C. reinhardtii* structures (Table 1). The binding affinity of the TDS in these two modes appears to be controlled by a single residue change Leu↔Phe at residue 81 of subunit IV in these two organisms, as a dramatic increase in the sensitivity of the b_6f complex to TDS and stigmatellin was obtained with mutation IV-L81F in *Synechococcus* sp. PCC 7002. It was inferred that the ring-in binding mode is responsible for the inhibitory effect. Therefore, the question arises: how does a Leu→Phe change at residue 81 of subunit IV dramatically increase the TDS binding affinity in the ring-in mode? One answer is that the aromat–aromat or van der Waals interactions between the Phe and TDS are critical for the stabilization of TDS in this orientation. Phe is, in fact, the most common residue at this position in the bc_1 complex. It is also located at the entrance to the Q_p pocket and in addition, is one of the few residues that is in close contact with all bound Q_p site inhibitors (stigmatellin, UHDBT, NQNO, famoxadone, myxothiazol, MOA-stilbene, and azoxystrobin) in the bovine bc_1 complex.[29] However, the natural presence of a Leu residue at this position in yeast does not impair the binding of stigmatellin in the ring-in mode,[22] and one stigmatellin per bc_1 complex was able to fully inhibit the bc_1 complex.[33] Although the binding affinity of TDS is three orders of magnitude weaker than stigmatellin in the bc_1 complex,[34] TDS is comparable to stigmatellin in its inhibition of the b_6f complex (Table 2). Therefore, other structure differences between the bc_1 and b_6f complexes at the Q_p site must be considered.

The cytochrome b_6f complex contains one chlorophyll *a* molecule per monomer. Its function is enigmatic, because no light reaction is required for the turnover of the complex.[35–38] As does the TDS tail, the chlorophyll phytol chain also resides in the Q_p-portal, resulting in a smaller free space of the Q_p-portal than that of the bc_1 complex.[1] This might explain why TDS can be as effective an inhibitor as stigmatellin in the b_6f complex because of its requirement of less space, although the latter has a more bulky hydrophobic tail. The chlorophyll phytol chain is in a similar bent-down conformation in the native and TDS-bound structures of the *M. laminosus* complex,[1] ruling out the possibility that the bent-down conformation is induced by TDS binding in the ring-out mode. Because of the absence of a native structure of the *C. reinhardtii* b_6f complex, it is not clear whether its bent-up conformation of the phytol chain is caused by TDS binding in the ring-in mode or whether it is a fixed conformation. The ring-in TDS tail might induce and stabilize the phytol chain in the bent-up conformation through van der Waals interactions. Alternatively, this bent-up conformation might be correlated with the presence of a Phe at residue 81 of subunit IV. In either case, it is expected that the mutation IV-L81F would also cause a similar tenfold decrease in the binding affinity of TDS in the ring-out mode because the concomitant bent-up conformation of phytol chain would displace the TDS binding in the ring-out mode by steric competition. Therefore, this L81F change in subunit IV would result in a dominant ring-in binding mode of TDS in green algae/higher plants although, in cyanobacteria, TDS preferably binds in a ring-out mode.

It is of interest that the major conformational difference between the bent-up and the bent-down phytol chains is at the start (C1–C4) near the ester group, which is close (3–4 Å) to residue 81 of subunit IV. In the superimposed structures, this C1–C4 of the bent-up phytol chain is 1–2 Å closer to IV-F81 than that of the bent-down conformation (Figure 3). Therefore, in addition to the direct aromat–aromat or van der Waals interactions with the TDS, residue 81 of subunit IV might also affect TDS binding through its interaction with the start (C1–C4) of the phytol chain (equation (1); Figure 7):

$$\frac{\text{bent-down}}{\text{phytol chain}} + \frac{\text{ring-out}}{\text{TDS}} \underset{\text{IV-F81L}}{\overset{\text{IV-L81F}}{\rightleftarrows}} \frac{\text{bent-up}}{\text{phytol chain}} + \frac{\text{ring-in}}{\text{TDS}} \quad (1)$$

Intermediate state of quinone translocation

The structures of respiratory and photosynthetic cytochrome *bc* complexes provide unique information on the pathway and mechanism of transfer of the small hydrophobic substrate, lipophilic quinone, between the bulk lipid phase and the reaction sites in the membrane–protein complex. The inter-monomer quinone exchange cavity facilitates the movement of the lipophilic quinone molecules between the bulk lipid phase and the intra-membrane cytochrome *bc* complex, and allows exchange of reaction products between the Q_p and Q_n sites in the complex.[1,18] It had been

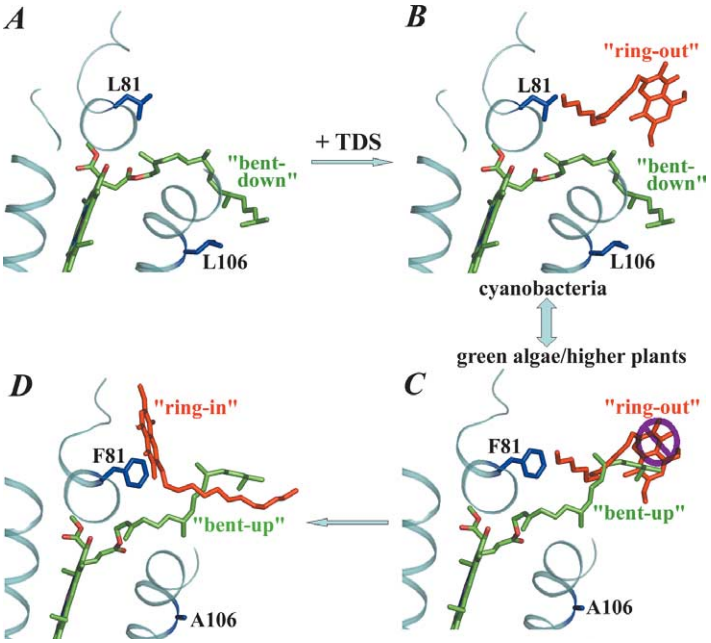

Figure 7. Model for the control of the TDS binding in the ring-in and ring-out modes by interactions between the residue 81 of subunit IV and the chlorophyll phytol chain. A, In cyanobacteria in which the residue 81 of subunit IV is a Leu, the chlorophyll phytol chain adopts a bent-down conformation, and (B) the TDS preferably binds in the ring-out mode. C and D, When Leu81 in cyanobacteria is changed to a Phe in green algae/higher plants, the chlorophyll phytol chain is induced into a bent-up conformation, which would displace the TDS binding in the ring-out binding mode (N.B., purple stop sign) and stabilize the TDS binding in the ring-in mode. Leu106 of subunit IV in cyanobacteria may have a role in stabilization of the bent-down conformation of the chlorophyll phytol chain, which is replaced by a small residue Ala in green algae/higher plants. Mutation of this Leu residue to Ala in *Synechococcus* resulted in a 40% decrease in the electron transfer activity, although the inhibitor sensitivity of TDS and stigmatellin was not significantly changed (data not shown).

estimated in the *Rh. sphaeroides* bc_1 complex that the exchange of quinol and quinone at the Q_p site is rapid ($\tau \leq 200$ μs).[39] During this process, the quinol/quinone must move between the quinone-exchange cavity and the Q_p pocket, and may transiently bind to many sites. The ring-out binding mode seen in the *M. laminosus* b_6f structure may represent one of the intermediate states for the movement of physiological quinone or its analogues between the quinone exchange cavity and the Q_p pocket. To our knowledge, this is the first observation of a second binding site of a lipophilic inhibitor or substrate that is related to its movement to/from the active binding site in the membrane–protein complex. Together with the n-side bound states of native quinones or Q_n site inhibitors and the p-side bound states of various other Q_p site inhibitors, more than a dozen different positions of quinone/ol or quinone analogues can be documented in the total set of b_6f and bc_1 structures.[1,2,18,19,21,22,27,28] By comparison, in the resolved X-ray structures of membrane transporter proteins, lactose permease,[40] glycerol-3-phosphate transporter,[41] long-chain fatty acid transporter FadL,[42] multidrug efflux transporters,[43–45] and ATP-binding cassette (ABC) transporters,[46,47] no more than one binding site of a substrate or analogue has been found.

Materials and Methods

Growth of cultures

Synechococcus sp. PCC 7002 wild-type and mutant strains were grown in medium A,[48] supplemented with 100 μg ml^{-1} spectinomycin for strains, WT^S, ISP-L111A, and ISP-L111Y, and with additional 50 μg ml^{-1} kanomycin for strains, WT^{HSK}, IV-L81F, IV-L81A, b_6-L193A. Liquid cultures were grown at 38 °C under cool-white fluorescent illumination at a light intensity of ~100 μEinstein m^{-2} s^{-1}, bubbled with air supplemented with ~2.0% (v/v) CO_2.

Site-directed mutagenesis and plasmid construction

A PCR-based site-directed mutagenesis method (Stratagene) was performed as in a previous report.[49] The presence of mutations and the intactness of the remainder of the *petCA* or *petBD* genes on plasmids and in the *Synechococcus* genome were analyzed by DNA sequencing. To construct plasmids for the site-directed mutagenesis on cytochrome b_6 gene *petB* and subunit IV gene *petD*, genomic DNA of *Synechococcus* sp. PCC7002 was isolated as described.[50] A 2.7 kb DNA fragment, encompassing the *petBD* operon and its 0.45 kb 5′ and 1.0 kb 3′ flanking sequence, was amplified from the genomic DNA by PCR with *pfu* polymerase, forward primer GGGTTTTGAGGGGCCGCTTC, and reverse primer (underlined, introduced EcoRI site) GAGAATTC AAATCGCCAACCAGGATG, and cloned into the HincII and EcoRI sites of vector pUC19 to generate plasmid pUCBD (5.3 kb). Plasmid pBD1 was derived through introduction of three restriction sites on pUCBD in non-coding regions by site-directed mutagenesis with the following primers (complementary primers not shown; restriction sites underlined): (i) a unique PacI site at 70 bp upstream of petB ORF, GCCCGATAATCCTGTTAATTAA CCACTTGACAGAGCAAGC; (ii) a second HindIII site in the non-coding region between the *petB* and *petD* ORFs, GGTTTTCCGTTTGCTCAAAACAAGCTTCTTGTTGAG GA GAACTTTTACTC; (iii) a unique EcoRV site at 200 bp downstream of *petD* ORF, GGCTCCGGCTAAAC GATATCGATCGCCTTTTTTGTTAGG. A 1.1 kb Kan^R cassette, which encodes kanamycin nucleotidyl-transferase and confers kanamycin resistance to the host strains, was excised from plasmid pRL448 (a kind gift from Dr

L.A. Sherman, Purdue University) by SmaI and ligated to the EcoRV site of pBD1 to generate plasmid pBD2. Mutational changes of *petB* and *petD* were first constructed on plasmid pBD1 by site-directed mutagenesis, and then the pBD2 mutant was constructed to transform the *Synechococcus* sp. PCC 7002 cells. Mutants of the ISP gene *petC1* were constructed according to our previous report.[26] Mutations were made by site-directed mutagenesis with the following primers (complementary primers not shown; mutation sites are underlined): ISP-L111A, C AAC GCC ATC TGT ACC CAC GCT GGT TGT GTC GTC CCT TGG; ISP-L111Y, C AAC GCC ATC TGT ACC CAC TAT GGT TGT GTC GTC CCT TGG; IV-L81F, G CCG GAG TGG TAC TTC TAC CCC GTC TTC C; IV-L81A, G CCG GAG TGG TAC GCC TAC CCC GTC TTC C; b_6-L193A, CTA ACC CGT TTC TAC AGT GCT CAT ACT TTT GTT TTA CCT TGG.

Transformation of *Synechococcus* cells and screening of complete segregants

To generate strains, WT^S, ISP-L111A, and ISP-L111Y, the wild-type and corresponding variants of plasmid pCA1 were transformed into *Synechococcus* sp. PCC 7002 wild-type cells, and the complete segregants were screened as described.[26] To generate strains, WT^{HSK}, IV-L81F, IV-L81A, and b_6-L193A, a WT^{HS} strain which has a 6His-tag at the C terminus of cytochrome *f* and is resistant to spectinomycin (J.Y & W.A.C., unpublished results), was used as the receptor of the WT and corresponding variants of plasmid pBD2. Transformation was performed as described.[26] Transformants were selected on plates supplemented with 50 μg ml^{-1} kanamycin and 100 μg ml^{-1} spectinomycin. The primary screen for the complete segregants of subunit IV mutants was performed by amplification of the whole *petBD* operon from the genomic DNA of the transformants by PCR, using primers TATCCGCCAAAAAGCCCG and ATCGCCA TCGTTTAGCCG, and by subsequent restriction analysis of the PCR product (1.54 kb) by HindIII digestion. Similarly, the primary screen for the complete segregants of cytochrome b_6 mutants was performed by amplification of the whole *petB* ORF with its ~0.5 kb 5′ and 0.3 kb 3′ flanking sequence from the genomic DNA of the transformants by PCR with primers GTAGGCTTGACT GACGTAACGC and ATCTGGAAGACGGGGTAGAGG, and by subsequent restriction analysis of the PCR product (1.36 kb) by PacI digestion. Complete digestion of the PCR product by HindIII for the former, and by PacI for the latter, indicated complete segregation and absence of the wild-type allele in the *Synechococcus* genome. The presence of desired mutations in the *petC1*, *petB* and *petD* genes of *Synechococcus* genome and their complete segregation from the wild-type alleles, were confirmed by sequencing of the PCR products that can be completely digested by HindIII or PacI.

Flash kinetic spectroscopy

Electron transfer activity of the cytochrome b_6f complex *in vivo* was assayed in terms of the measurable indicator of the rate-limiting step in the electron transfer chain, the reduction of cytochromes *f* and c_6. The flash-induced oxidation and re-reduction of cytochrome *f* and c_6 were monitored in their α-absorbance band region ($\Delta A_{556-540\ nm}$) using the laboratory-built single-beam spectrometer described.[49] Short saturating actinic flashes, which had a half-peak width of 5 μs, were produced by a xenon flash lamp filtered with red blocking filters (two Corning 2-58 filters, $\lambda > 600$ nm) and directed on the sample at right angle to the measuring beam. To measure the electron transfer activity of the b_6f complex under successive turnovers condition, double flashes (dark time between two successive flashes, 100 ms) were employed to trigger multiple turnovers of the complexes and the kinetics of the second flash-induced re-reduction of cytochrome f/c_6 was used to obtain the electron transfer activity of the b_6f complex in this study. To improve the signal-to-noise ratio, 36 double flash-induced absorbance changes were averaged at frequencies of 0.1–0.3 Hz. *Synechococcus* cells were harvested in late log phase and kept in darkness. Prior to measurement, cells were suspended at 5 μM chlorophyll in a reaction medium consisting of 5 mM Hepes (pH 7.5), 10 mM NaCl, and 10 mM $NaHCO_3$. Carbonyl cyanide *p*-trifluoromethoxyphenylhydrazone (FCCP) (10 μM) was added to eliminate the trans-membrane electrochemical potential. In cyanobacteria, the plastoquinone pool and cytochrome b_6f complex are shared by photosynthetic and respiratory electron transport chains. To minimize variation in the redox state of the PQ pool in the dark, 1.0 mM KCN was added to the cell suspension and incubated for one minute at room temperature to block respiration. Inhibitors were added to the cell suspension from stock solutions in dimethyl sulfoxide (final DMSO concentration ≤0.5%) and incubated for one minute prior to measurements.

Acknowledgements

This study was supported by NIH grant GM-38323. We are grateful to H. Zhang, G. Kurisu, and J. L. Smith for helpful advice and discussions, and to P. Rich for a gift of TDS. The crystallographic analysis, on which this study is based, was carried out on beam-line SBC-19 at the Advanced Photon Source, Argonne National Laboratory, which was supported by the US Department of Energy (DOE grant W31-109-ENG-389), and at Spring-8 BL44XU (Hyogo, Japan).

Supplementary Data

Supplementary data associated with this article can be found, in the online version, at doi:10.1016/j.jmb.2004.09.053

References

1. Kurisu, G., Zhang, H., Smith, J. L. & Cramer, W. A. (2003). Structure of the cytochrome b_6f complex of oxygenic photosynthesis: tuning the cavity. *Science*, **302**, 1009–1014.
2. Stroebel, D., Choquet, Y., Popot, J. L. & Picot, D. (2003). An atypical haem in the cytochrome b_6f complex. *Nature*, **426**, 413–418.
3. Allen, J. F. (2004). Cytochrome b_6f: structure for signalling and vectorial metabolism. *Trends Plant Sci.* **9**, 130–137.

4. Cramer, W. A., Zhang, H., Yan, J., Kurisu, G. & Smith, J. L. (2004). Evolution of photosynthesis: time-independent structure of the cytochrome b_6f complex. *Biochemistry*, **43**, 5921–5929.
5. Smith, J. L., Zhang, H., Yan, J., Kurisu, G. & Cramer, W. A. (2004). Cytochrome *bc* complexes: a common core of structure and function surrounded by diversity in the outlying provinces. *Curr. Opin. Struct. Biol.* **14**, 432–439.
6. Velthuys, B. R. (1979). Electron flow through plastoquinone and cytochrome b_6 and *f* in chloroplasts. *Proc. Natl Acad. Sci. USA*, **76**, 2765–2769.
7. Prince, R. C., Matsuura, K., Hurt, E., Hauska, G. & Dutton, P. L. (1982). Reduction of cytochromes b_6 and *f* in isolated plastoquinol-plastocyanin oxidoreductase driven by photochemical reaction centers from *Rhodopseudomonas sphaeroides*. *J. Biol. Chem.* **257**, 3379–3381.
8. Rich, P. R. (1986). A perspective on Q-cycles. *J. Bioenerg. Biomembr.* **18**, 145–156.
9. Joliot, P. & Joliot, A. (1986). Proton pumping and electron transfer in the cytochrome *b/f* complex of algae. *Biochim. Biophys. Acta*, **849**, 211–222.
10. Joliot, P. & Joliot, A. (1994). Mechanism of electron transfer in the cytochrome *b/f* complex of algae: evidence for a semiquinone cycle. *Proc. Natl Acad. Sci. USA*, **91**, 1034–1038.
11. Osyczka, A., Moser, C. C., Daldal, F. & Dutton, P. L. (2004). Reversible redox energy coupling in electron transfer chains. *Nature*, **427**, 607–612.
12. Girvin, M. E. & Cramer, W. A. (1984). A redox study of the electron transport pathway responsible for generation of the slow electrochromic phase in chloroplasts. *Biochim. Biophys. Acta*, **767**, 29–38.
13. Kramer, D. M. & Crofts, A. R. (1994). Re-examination of the properties and function of the *b* cytochrome of the thylakoid cytochrome *bf* complex. *Biochim. Biophys. Acta*, **1184**, 193–201.
14. Crofts, A. R. (2004). The cytochrome bc_1 complex: function in the context of structure. *Annu. Rev. Physiol.* **66**, 689–733.
15. Soriano, G. M., Ponamarev, M. V., Carrell, C. J., Xia, D., Smith, J. L. & Cramer, W. A. (1999). Comparison of the cytochrome bc_1 complex with the anticipated structure of the cytochrome b_6f complex: Le plus ca change le plus c'est la meme chose. *J. Bioenerg. Biomembr.* **31**, 201–213.
16. Berry, E. A., Guergova-Kuras, M., Huang, L. S. & Crofts, A. R. (2000). Structure and function of cytochrome *bc* complexes. *Annu. Rev. Biochem.* **69**, 1005–1075.
17. Widger, W. R., Cramer, W. A., Herrmann, R. G. & Trebst, A. (1984). Sequence homology and structural similarity between cytochrome *b* of mitochondrial complex III and the chloroplast b_6-f complex: position of the cytochrome *b* hemes in the membrane. *Proc. Natl Acad. Sci. USA*, **81**, 674–678.
18. Xia, D., Yu, C. A., Kim, H., Xia, J. Z., Kachurin, A. M., Zhang, L. *et al*. (1997). Crystal structure of the cytochrome bc_1 complex from bovine heart mitochondria. *Science*, **277**, 60–66.
19. Zhang, Z., Huang, L., Shulmeister, V. M., Chi, Y. I., Kim, K. K., Hung, L. W. *et al*. (1998). Electron transfer by domain movement in cytochrome bc_1. *Nature*, **392**, 677–684.
20. Iwata, S., Lee, J. W., Okada, K., Lee, J. K., Iwata, M., Rasmussen, B. *et al*. (1998). Complete structure of the 11-subunit bovine mitochondrial cytochrome bc_1 complex. *Science*, **281**, 64–71.
21. Kim, H., Xia, D., Yu, C. A., Xia, J. Z., Kachurin, A. M., Zhang, L. *et al*. (1998). Inhibitor binding changes domain mobility in the iron–sulfur protein of the mitochondrial bc_1 complex from bovine heart. *Proc. Natl Acad. Sci. USA*, **95**, 8026–8033.
22. Hunte, C., Koepke, J., Lange, C., Rossmanith, T. & Michel, H. (2000). Structure at 2.3 Å resolution of the cytochrome bc_1 complex from the yeast *Saccharomyces cerevisiae* co-crystallized with an antibody Fv fragment. *Structure*, **8**, 669–684.
23. Knoll, A. H. (2003). *Life on a Young Planet: the First Three Billion Years of Evolution on Earth*. Princeton University Press, Princeton, NJ.
24. Brasseur, G., Sled, V., Liebl, U., Ohnishi, T. & Daldal, F. (1997). The amino-terminal portion of the Rieske iron–sulfur protein contributes to the ubihydroquinone oxidation site catalysis of the *Rhodobacter capsulatus* bc_1 complex. *Biochemistry*, **36**, 11685–11696.
25. Liebl, U., Sled, V., Brasseur, G., Ohnishi, T. & Daldal, F. (1997). Conserved non-liganding residues of the *Rhodobacter capsulatus* Rieske iron–sulfur protein of the bc_1 complex are essential for protein structure, properties of the [2Fe–2S] cluster, and communication with the quinone pool. *Biochemistry*, **36**, 11675–11684.
26. Yan, J. & Cramer, W. A. (2003). Functional insensitivity of the cytochrome b_6f complex to structure changes in the hinge region of the Rieske iron–sulfur protein. *J. Biol. Chem.* **278**, 20925–20933.
27. Gao, X., Wen, X., Esser, L., Quinn, B., Yu, L., Yu, C. A. & Xia, D. (2003). Structural basis for the quinone reduction in the bc_1 complex: a comparative analysis of crystal structures of mitochondrial cytochrome bc_1 with bound substrate and inhibitors at the Qi site. *Biochemistry*, **42**, 9067–9080.
28. Palsdottir, H., Lojero, C. G., Trumpower, B. L. & Hunte, C. (2003). Structure of the yeast cytochrome bc_1 complex with a hydroxyquinone anion Q_o site inhibitor bound. *J. Biol. Chem.* **278**, 31303–31311.
29. Esser, L., Quinn, B., Li, Y. F., Zhang, M., Elberry, M., Yu, L. *et al*. (2004). Crystallographic studies of quinol oxidation site inhibitors: a modified classification of inhibitors for the cytochrome bc_1 complex. *J. Mol. Biol.* **341**, 281–302.
30. Link, T. A. (1997). The role of the "Rieske" iron sulfur protein in the hydroquinone oxidation (Q(P)) site of the cytochrome bc_1 complex. The "proton-gated affinity change" mechanism. *FEBS Letters*, **412**, 257–264.
31. Crofts, A. R., Guergova-Kuras, M., Huang, L., Kuras, R., Zhang, Z. & Berry, E. A. (1999). Mechanism of ubiquinol oxidation by the bc_1 complex: role of the iron sulfur protein and its mobility. *Biochemistry*, **38**, 15791–15806.
32. Samoilova, R. I., Kolling, D., Uzawa, T., Iwasaki, T., Crofts, A. R. & Dikanov, S. A. (2002). The interaction of the Rieske iron–sulfur protein with occupants of the Q_o-site of the bc_1 complex, probed by electron spin echo envelope modulation. *J. Biol. Chem.* **277**, 4605–4608.
33. Gutierrez-Cirlos, E. B. & Trumpower, B. L. (2002). Inhibitory analogs of ubiquinol act anti-cooperatively on the Yeast cytochrome bc_1 complex. Evidence for an alternating, half-of-the-sites mechanism of ubiquinol oxidation. *J. Biol. Chem.* **277**, 1195–1202.
34. Ohnishi, T., Brandt, U. & von Jagow, G. (1988). Studies on the effect of stigmatellin derivatives on cytochrome *b* and the Rieske iron–sulfur cluster of cytochrome c reductase from bovine heart mitochondria. *Eur. J. Biochem.* **176**, 385–389.

35. Huang, D., Everly, R. M., Cheng, R. H., Heymann, J. B., Schagger, H., Sled, V. *et al*. (1994). Characterization of the chloroplast cytochrome b_6f complex as a structural and functional dimer. *Biochemistry*, **33**, 4401–4409.
36. Pierre, Y., Breyton, C., Lemoine, Y., Robert, B., Vernotte, C. & Popot, J. L. (1997). On the presence and role of a molecule of chlorophyll a in the cytochrome b_6f complex. *J. Biol. Chem.* **272**, 21901–21908.
37. Peterman, E. J., Wenk, S. O., Pullerits, T., Palsson, L. O., van Grondelle, R., Dekker, J. P. *et al*. (1998). Fluorescence and absorption spectroscopy of the weakly fluorescent chlorophyll a in cytochrome b_6f of Synechocystis PCC6803. *Biophys. J.* **75**, 389–398.
38. Zhang, H., Huang, D. & Cramer, W. A. (1999). Stoichiometrically bound beta-carotene in the cytochrome b_6f complex of oxygenic photosynthesis protects against oxygen damage. *J. Biol. Chem.* **274**, 1581–1587.
39. Crofts, A. R., Shinkarev, V. P., Kolling, D. R. & Hong, S. (2003). The modified Q-cycle explains the apparent mismatch between the kinetics of reduction of cytochromes c_1 and b_H in the bc_1 complex. *J. Biol. Chem.* **278**, 36191–36201.
40. Abramson, J., Smirnova, I., Kasho, V., Verner, G., Kaback, H. R. & Iwata, S. (2003). Structure and mechanism of the lactose permease of *Escherichia coli*. *Science*, **301**, 610–615.
41. Huang, Y., Lemieux, M. J., Song, J., Auer, M. & Wang, D. N. (2003). Structure and mechanism of the glycerol-3-phosphate transporter from *Escherichia coli*. *Science*, **301**, 616–620.
42. van den Berg, B., Black, P. N., Clemons, W. M. & Rapoport, T. A. (2004). Crystal structure of the long-chain fatty acid transporter FadL. *Science*, **304**, 1506–1509.
43. Murakami, S., Nakashima, R., Yamashita, E. & Yamaguchi, A. (2002). Crystal structure of bacterial multidrug efflux transporter AcrB. *Nature*, **419**, 587–593.
44. Yu, E. W., McDermott, G., Zgurskaya, H. I., Nikaido, H. & Koshland, D. E. (2003). Structural basis of multiple drug-binding capacity of the AcrB multidrug efflux pump. *Science*, **300**, 976–980.
45. Ma, C. & Chang, G. (2004). Structure of the multidrug resistance efflux transporter EmrE from *Escherichia coli*. *Proc. Natl Acad. Sci. USA*, **101**, 2852–2857.
46. Chang, G. (2003). Structure of MsbA from Vibrio cholera: a multidrug resistance ABC transporter homolog in a closed conformation. *J. Mol. Biol.* **330**, 419–430.
47. Locher, K. P., Lee, A. T. & Rees, D. C. (2002). The *E. coli* BtuCD structure: a framework for ABC transporter architecture and mechanism. *Science*, **296**, 1091–1098.
48. Buzby, J. S., Porter, R. D. & Stevens, S. E. (1985). Expression of the *Escherichia coli* lacZ gene on a plasmid vector in a cyanobacterium. *Science*, **230**, 805–807.
49. Ponamarev, M. V. & Cramer, W. A. (1998). Perturbation of the internal water chain in cytochrome *f* of oxygenic photosynthesis: loss of the concerted reduction of cytochromes *f* and b_6. *Biochemistry*, **37**, 17199–17208.
50. Wu, X., Zarka, A. & Boussiba, S. (2000). A simplified protocol for preparing DNA from filamentous cyanobacteria. *Plant Mol. Biol. Rep.* **18**, 385–392.

Edited by I. B. Holland

(Received 27 June 2004; received in revised form 21 September 2004; accepted 21 September 2004)